International Journal of Luminescence and Applications (ISSN: 2277-6362)
Vol. 7, No. 3-4, October - December 2017. Article ID: 246. pp.434-445.

Synthesis and Characterization of $BaAlSi_5O_2N_7$:Tb Nitride Based Phosphor

S.A. Fartode[1] and **S.J. Dhoble[2*]**

[1]*Department of Applied Physics, Dr.Babasaheb Ambedkar College of Engineering and Research, Nagpur, India*
[2]*Department of Physics, RTM Nagpur University, Nagpur, India.*

Abstract— *This paper discusses synthesis, photoluminescence, mechanoluminescence and thermoluminescence properties of Tb^{3+} activated $BaAlSi_5O_2N_7$ oxinitride phosphor. The material was synthesized through modified two step high temperature solid state diffusion technique. The Tb^{3+} activated $BaAlSi_5O_2N_7$ material shows efficient emission at 490 nm, 545 nm, 552 nm, 584 nm and 617 nm due to $^5D_3$ and $^5D_4$ to ^7F_J (J=3,4,5 &6) transition of Tb^{3+} ion, under excitation at 270 nm.*

The mechanoluminescence (ML) in Tb^{3+} doped $BaAlSi_5O_2N_7$ shows that the time corresponding to peaks shifts towards shorter time values with increasing impact velocity. It is also seen that the total ML intensity I_{Total} initially increases with the impact velocity and attains a saturation value for higher values of the impact velocity. The peak ML intensity I_m and total ML intensity I_T increases quardratically with the applied load and impact velocity. This fundamental work might be important in developing new luminescent devices applicable for ML sensors and dosimeter.

In TL study, *γ-irradiated TL glow curve of $BaAlSi_5O_2N_7$: Tb^{3+} phosphor shows four well defined*

peaks at 420K, 446K, 473K and 507K indicating that four type of trap is being activated within the particular temperature range. The position of glow peak was estimated by Tm-Tstop method. The trapping parameters associated with the prominent glow peaks of $BaAlSi_5O_2N_7$: Tb^{3+} are ***calculated using Chen's peak shape and initial rise method****.*

Keywords— *$BaAlSi_5O_2N_7$, photoluminescence, phosphor, mechanoluminescence, solid state diffusion method, thermoluminescence.*

1. INTRODUCTION

The solid-state lighting industry witnessed significant improvement due to rare earth activated luminescent phosphors. In 1996, Nichia Chemical Co. invented white LEDs prepared by coating blue InGaN LED chip with yellow $Y_3Al_5O_{12}$:Ce phosphor [1]. The white light emitting diodes (W-LEDs) have high power efficiency, long lifetime, nonpolluting and flexibility in the design process over the conventional incandescent and fluorescent lamps [2,3].The combination of UV LED with RGB phosphors may be considered a navigator in the development of solid-state lighting due to its attributes like high efficiency and high chromatic stability [4]. A host material combined with suitable activator produce phosphors. Generally aluminate, nitride, sulphate, sulphide etc.are used as host materials due to good optical, mechanical, and thermal properties[5]. Recently photoluminescence properties of aluminosilicon nitride/oxynitride doped with novel rare-earth have been extensively explored.

To cope up with the high demand of white LED lighting, Eu^{2+}, Ce^{3+} and Tb^{3+} activated aluminosilicon nitride-based luminescent materials have been rapidly developed [6-13]. Due to the presence of nitrogen in the lattices, silicon oxynitride/nitride-based compounds have unique structural features [14–18]. Therefore for Eu^{2+} and Tb^{3+} activator ions, appropriate difference in the luminescence properties is expected. The excitation and emission bands of these ions can be shifted to lower energies due to high degree of covalent bonding and large crystal field splitting of 5d excited levels [19]. The unique optical behavior is shown by Eu^{3+}, Tb^{3+}, Dy^{3+} and Tm^{3+} ions when doped into host material. The electronic transitions occurring within the partially filled 4f energy shell of the lanthanide series contributes to the luminescence of these ions [20].The efficient phosphors were developed by using remarkable narrow-band emission properties of the rare earth metal ions [21]. Particularly for efficient blue–green emissions, Tb^{3+} ions are used as activators. This begins from the transitions of $^5D_3$ and $^5D_4$ excited states to ^7F_J (J=0, 1… 6) ground states of Tb^{3+} ions. For UV radiation excitation, Tb^{3+} ions are raised to higher $4f^75d^1$ level from $4f^8$ and afterward raised to $^5D_3$ or $^5D_4$ excited states [22]. Tb^{3+} activated phosphors have been widely used in various applications such as X-ray intensifying screens, three-band fluorescent lamps and projection television tubes [23].

Mechanoluminescence (ML) is photoemission from some materials due to an applied mechanical simulation. These mechanical actions could include friction, pressure, bending, erasing or rubbing, fracture and shocking etc.

* *Corresponding author: sjdhoble@rediffmail.com*

For a long time the interest in ML has been academic in nature, with the majority of works either reporting new ML materials, detailing methods for quantitative generating and measuring ML, recording ML spectra and suggesting mechanisms underlying the deformation and fracture-induced excitation processes. Many efforts have been undertaken to make the solar energy more available in recent years. One of the proposals is to use the long-lasting phosphorescence (LLP) materials to absorb and store sunlight energy in daytime and then emit slowly at night for illumination purposes [24]. As a category of ML materials, elastico mechanoluminescence (EML) materials present an accurate linearity of ML intensity against load in the elastic region in addition to mechano-optical conversion [25].

Previous researches have indicated that the developed EML materials belong to the defect controlled type piezoelectric materials and the EML mechanism has been explained using the piezoelectrically induced carrier de-trapping model [25-31]. Consequently the above mentioned EML performance should be closely related to the concentration and depth of trap levels. On one hand the EML intensity is mainly influenced by the concentration of trap levels. If the concentration of trap levels whose depths are suitable for EML is relatively higher, more trapped carriers are released which then recombine with the luminescence centers under the applied stress to give an intense EML as in the cases of $Sr_{n+1}Sn_nO_{3n+1}:Sm^{3+}$ (n = 1, 2, ∞) and $(Ca,Sr,Ba)Si_2O_2N_2:Eu^{2+}$ [29,30]. On the other hand the depth of trap levels is responsible for load threshold and the measurement range of dynamic load. e.g. $SrAl_2O_4:Eu^{2+}$ exhibits an intense EML even under the application of a weak mechanical force such as that generated by scratching the material with a finger. The shallow trap levels (0.2 ± 0.1 eV) are one of the most important reasons for its sensitivity to the weak load [28]. Nevertheless it should be also pointed out that if there are only shallow (accessible) or less deep trap levels, the carriers in the traps can be released and then be emptied under the weak load which results in absence or weakness of EML under the strong load. On the contrary, if there are only deep or less shallow trap levels, the energy necessary for the carriers to release from the traps is so high that the trapped carriers cannot be excited by the weak load, resulting in a high load threshold for EML. Therefore to search and design novel EML materials with suitable multiple trap levels is an effective and promising method to obtain the excellent EML performance.The simple and consistent technique for dosimetry of high-energy radiation is thermoluminescence. The number of high-energy particles passing through the material decides the number of electron/hole traps generated during the irradiation. The traps are generally stable at room temperature. The traps should be stimulated by thermal energy so that recombination takes place. The TL emission is traced as a function of temperature. The intensity of light emitted by phosphor is proportional to the radiation doses given to it. There are several commercially available TLD phosphors such as LiF:Mg,Ti (TLD-100), LiF:Mg,Cu,P (TLD-700), CaF_2:Dy (TLD-200), CaF_2:Tm (TLD-300). However one or the other drawback is associated with every phosphor [32]. Thermoluminescence dosimetry (TLD) is one of the well-known dosimetric techniques having wide applications in various areas such as clinical, personal and environmental dosimetry. The important and convenient method of investigating the nature of traps and trapping levels in crystals is thermally stimulated luminescence (TL). In general all thermoluminescent materials also show ML during their deformation [33]. This paper reports photoluminescence, mechanoluminescence and thermoluminescence properties of Tb^{3+} activated $BaAlSi_5O_2N_7$ oxinitride phosphor.

2. EXPERIMENTAL

$BaAlSi_5O_2N_7:Tb^{3+}$ phosphors were synthesized by high temperature solid-state diffusion method. The starting materials were high purity $BaCO_3$ (Merck, >99.0%), α-Si_3N_4 powder, $Al(NO_3)_3$, Al_2O_3 and Tb_2O_3 of AR grade. The appropriate amounts of starting materials were mixed and ground together in an agate mortar. The powder mixtures were then transferred into crucibles. Subsequently those powder mixtures were fired in a furnace at 400^0C for 1 hr and after crushing again fired in a horizontal tube furnace (muffle furnace) at 800^0C for 24 hr in open air atmosphere. Samples were gradually cooled down to the room temperature in the furnace. The samples were again fired in a furnace at 1200^0C for four hrs and pulverized for further measurements.

All measurements were performed on finely ground samples which were analyzed by X-ray powder diffraction. All the XRD measurements were performed at room temperature in air. The composition and phase purity of products were measured by powder X-ray diffraction (XRD) analysis with an X'Pert PRO diffractometer with Cu-Kα radiation (λ= $1.54060A^0$) operated at 45 kV and 40 mA. The XRD data were collected in a 2θ range from 10^0 to 80^0. The photoluminescence (PL) emission spectra of the sample were recorded using fluorescence spectrometer (Hitachi F-4000). The same amount of sample was used in each case. The emission and excitation spectra were recorded using spectral slit width of 1.5 nm. The experimental setup used for impulsive excitation of mechanoluminescence (ML) in γ- irradiated Tb doped $BaAlSi_5O_2N_7$ phosphor is as follows. The sample was placed on upper surface of a transparent Lucite plate. It was covered with a thin aluminum foil and fixed with adhesive tape. The load of different masses was dropped from different heights and the impact velocity of the load was changed. For taking ML measurement the phosphor was placed on a transparent Lucite plate inside a sampler

holder below the guiding cylinder and the luminescence was monitored below the transparent plate using an RCA 931A photomultiplier tube connected to a storage oscilloscope (SCINTIFIC HM-205). The photomultiplier housing was made of thick soft iron to provide a shielding from light and magnetic field. The slit arrangement at the window was provided to adjust the size of the window according to the incident beam. The ML intensity was monitored by photomultiplier tube whose output was fed to one channel of storage oscilloscope. For determining the peak intensity, peak position, rise and decay time of ML trace on the oscilloscope screen was recorded on tracing paper. The TL glow curve was recorded using TL reader (Nucleonix TL 1009I) by heating a sample with a heating rate 5^0C/s

3. RESULTS AND DISCUSSION

3.1 Structural Studies of $BaAlSi_5O_2N_7$ Host Phosphor

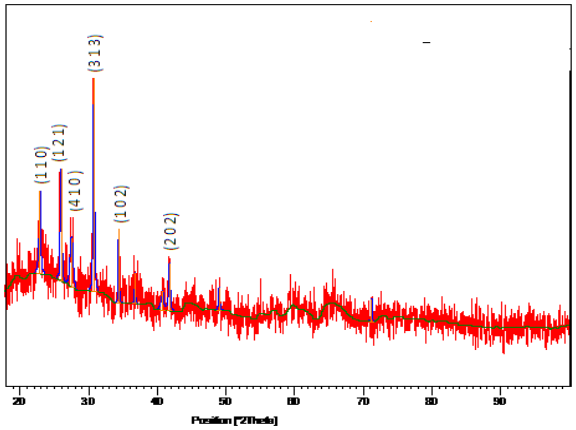

Fig. 1: XRD pattern of $BaAlSi_5O_2N_7$

Fig.1 shows the XRD pattern of $BaAlSi_5O_2N_7$ sample [57]. The XRD pattern of the prepared sample matched with the XRD pattern reported by Duan *et al*. [34]. However some minor peaks are found in the XRD spectrum which may be due to noise contributed by experimental errors. The miller indices of major peaks of XRD are also shown in Fig.1.

3.2 FTIR of $BaAlSi_5O_2N_7$:Tb^{3+}

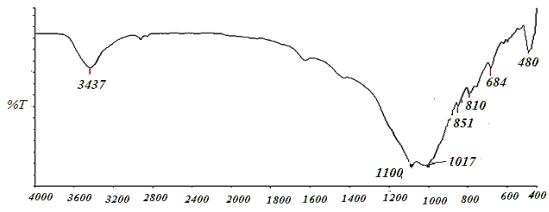

Fig. 2: FTIR spectra of $BaAlSi_5O_2N_7$:Tb^{3+}

In FTIR electromagnetic radiations are absorbed by the material in the infrared region of the spectrum which changes the vibration energy of molecule. Since usually all molecules possesses vibrations in form of stretching, bending, etc. the absorbed energy will be utilized in changing the energy levels associated with these. FTIR is the important tool for identification and structural analysis of organic compounds, natural products, polymers, etc.

When an infrared light interacts with the matter, chemical bonds will stretch, contract and bend. As a result, a chemical functional group tends to absorb infrared radiation in a specific wavenumber range regardless of the structure of the rest of the molecule [35]. The IR spectra of the sample in the wave number range from 4000 to 400 cm^{-1} as a function of percentage transmittance is reported in Fig.2

The IR spectrum of the sample has absorption band at 3437 cm^{-1} due to weak stretching of N-H bond. The absorption band at 1100 cm^{-1} and 810 cm^{-1} could be allocated to asymmetric stretching of Si-O-Si[36].The asymmetric stretching of M-ONO is found at 1017 cm^{-1}. The weak band at 851 cm^{-1} occurs due to stretching of N-O bond [35]. The band observed at 684 cm^{-1}, 599 cm^{-1} and 480 cm^{-1} are assigned to bending of M=O, M-NO_2, and Y-(0) N [35,36].

3.3 Luminescence of $BaAlSi_5O_2N_7$:Tb^{3+}

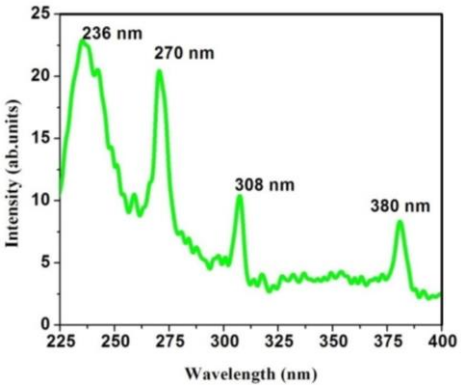

Fig. 3: Photoluminescence excitation spectrum of $BaAlSi_5O_2N_7$:Tb^{3+}

Under 270 nm excitation $BaAlSi_5O_2N_7$:Tb^{3+} emits bright blue green light (Fig.3). The emission spectrum(Fig.4) of Tb^{3+} in $BaAlSi_5O_2N_7$ is composed of two groups of lines in the wavelength range of 400-650 nm: one group in the range 490-650 nm corresponding to $^5D_4 \rightarrow {}^7F_J$ (J = 6,5,4,3) transitions of Tb^{3+} and other in range 400- 470 nm originating from the $^5D_3 \rightarrow {}^7F_J$ (J = 6,5,4,3,2,1,0) transitions of Tb^{3+}. The dominant one is $^5D_4 \rightarrow {}^7F_5$ at about 544 nm. The emission peak due to $^5D_4 \rightarrow {}^7F_5$ transition split into two peaks, one is at 544 nm and other at 552 nm due to crystal field effect[37]. It is well known that Tb^{3+} concentration affects the relative intensities of $^5D_4$ and $^5D_3$ emissions of Tb^{3+} activated samples. As the concentration of Tb^{3+} increases, the emission intensity increases from 0.05 mole% to 1 mole% and then decreases for 2 mole%. As the concentration of Tb^{3+} ion exceed 1 mole%, interaction between Tb^{3+} ions itself

takes place rather than having interaction between Tb^{3+} and host. This happens due to concentration quenching [38]. Normally a blue emission originating from $^5D_3$ level is mainly observed at a low Tb^{3+} concentration [37]. The critical transfer distance (R_0) from the concentration quenching can be calculated using the following formula [36]:

$$R_O = 2\left(\frac{3V}{4\pi X_c N}\right)^{\frac{1}{3}}$$

where R_0 is the critical concentration at which the quenching occurs, N is the number of Tb^{3+} ions in $BaAlSi_5O_2N_7$ unit cell and V is the volume of unit cell. By taking experimental and analytic values, the critical transfer distance in $BaAlSi_5O_2N_7$:Tb^{3+} phosphors is calculated to be 33.39 Å. The non radiative decay from $^5D_3$ state to $^5D_4$ state via cross relaxation ($^5D_3 \rightarrow {}^5D_4 \geq {}^7F_6 \rightarrow {}^7F_0$ and $^5D_3 \rightarrow {}^7F_0 \geq {}^7F_6 \rightarrow {}^5D_4$ is probable if the Tb^{3+} ions are present at short distances(Fig.4) and this results in a change from blue to green emission [35]. For a system where Tb^{3+} ions are distributed homogeneously, above change is observed when Tb^{3+} concentration is increased above the critical Tb^{3+} concentration for cross relaxation [38].

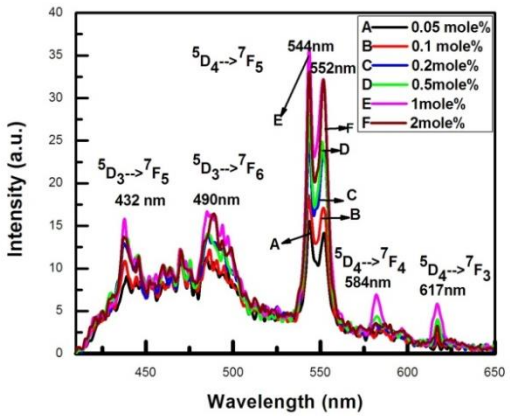

Fig. 4: Photoluminescence emission spectra of $BaAlSi_5O_2N_7$:Tb^{3+}

In excitation spectrum (Fig.3) some peaks are observed in the wavelength range of 230-400 nm which can be ascribed to the transitions between the energy levels within $4f^8$ configuration i.e. $^7F_6 \rightarrow {}^5D_3$ (≈ 380 nm) [37]. The peak at 270 nm in excitation spectrum of $BaAlSi_5O_2N_7$:Tb^{3+} may be attributed to $BaAlSi_5O_2N_7$ host absorption and terbium–oxygen charge-transfer respectively [40]

The ground states for Tb^{3+} ions are ^7F_J with $4f^8$ electron configuration. The transformation of one electron to 5d shell produced two $4f^75d^1$ excited state: the high spin state with ^9D_J configuration and the low spin state with ^7D_J configuration. But it was noticed that ^7D_J state is higher in energy than ^9D_J state. The Hund's rule suggested that the transitions between ^7F_J and ^7D_J are spin allowed while the transition between ^7F_J and ^9D_J are spin-forbidden. Therefore a specific host with Tb^{3+} ion exhibits two groups of f-d transition: at high energy the spin-allowed f-d transitions are strong and the spin-forbidden f-d transitions are weak at low energy [41]. The energy diagram of the luminescence of $BaAlSi_5O_2N_7$:Tb^{3+} phosphor is shown in Fig.5.

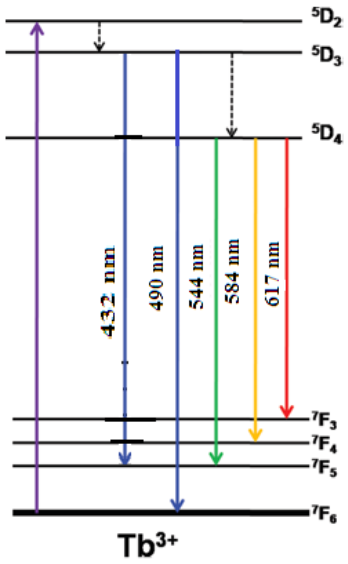

Fig. 5: A schematic diagram showing the transition of Tb^{3+} ions

4. MECHANOLUMINESCENE

ML glow curve for different impurity concentration, impact velocity, ML spectra, height and mass can be viewed in Figures 6, 7, 8, 9.10 and 11 respectively. The phosphor has a single glow curve with a single mechanoluminescence peak.

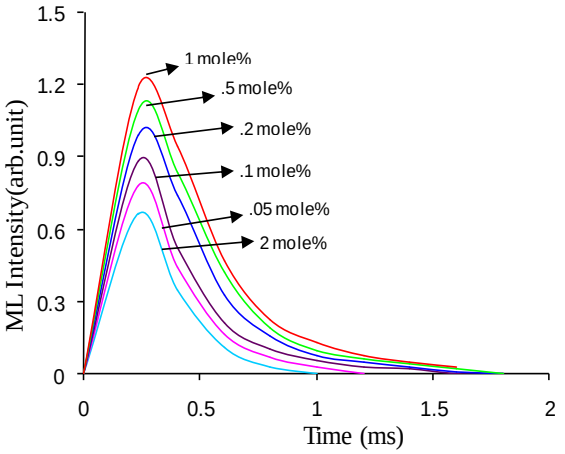

Fig. 6: Time dependence of ML intensity of $BaAlSi_5O_2N_7$:Tb samples for the different concentrations of impurities

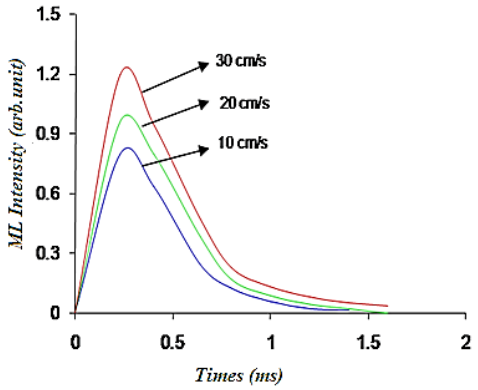

Fig. 7: ML glow curves of γ -irradiated $BaAlSi_5O_2N_7$:Tb samples for different impact velocities of the Piston

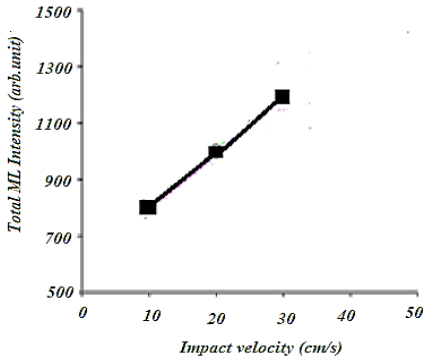

Fig. 8: Variation of total ML intensity with impact velocity for $BaAlSi_5O_2N_7$:Tb

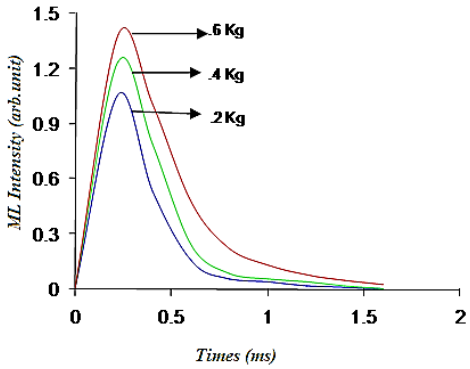

Fig. 9: ML intensity versus time curves of $BaAlSi_5O_2N_7$:Tb for different mass of the piston

Fig.6 shows the time dependence of ML intensity of $BaAlSi_5O_2N_7$:Tb sample for the different concentrations of impurities. It is clear that ML intensity increases with increasing concentration of impurities. For sample ML intensity was maximum for 1 mole% and for higher values of impurity concentration ML intensity decreases. This shows that the concentration quenching of luminescence centre may take place. ML intensity initially increased with time, attained an optimum value for a particular time and then decreased and finally disappeared for all the samples. However there is no considerable change in t_m (i.e. the time corresponding to ML peak).

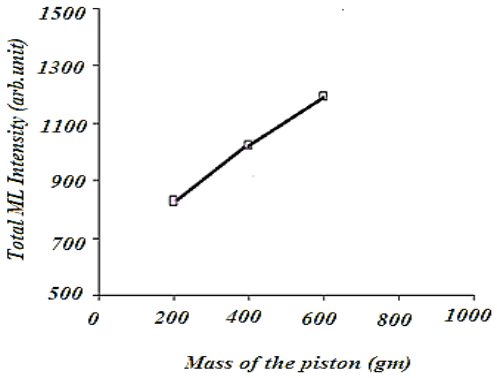

Fig. 10: Shows the variation of total ML intensity with mass of the piston for $BaAlSi_5O_2N_7$:Tb.

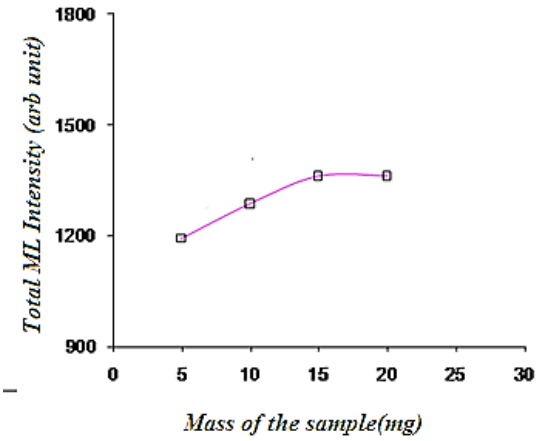

Fig. 11: Shows the ML glow curves for different mass of $BaAlSi_5O_2N_7$:Tb.

Fig.7 shows the ML glow curves of γ -irradiated rare earth Tb activated $BaAlSi_5O_2N_7$ samples for different impact velocities of the piston. In all concentrations maximum intensity is shown at 1 mole% of Tb activated barium based phosphor. It is seen that the ML intensity increases with increasing impact velocity. However the time corresponding to ML peak (t_m) shifts towards shorter time values with increasing impact velocity.

Fig.8 shows variation of total ML intensity with impact velocity. The total ML intensity of γ-irradiated Tb doped $BaAlSi_5O_2N_7$ increases linearly with increasing impact velocity of the piston of different mass and attains a maximum value for higher value of impact velocity. ML intensity increases almost linearly with increasing the mass (0.2 to 0.6 kg) of the piston. For recording ML the samples were irradiated with gamma-ray dose of 0.037 kGy at the dose rate of 0.32 kGy/hr. When the mass of the

piston increases, the number of newly created surface in the sample increases and thereby the ML intensity.

Fig.9 and Fig.10 shows the ML intensity versus time curves of samples for different mass of the piston dropped on $BaAlSi_5O_2N_7$: Tb. The ML intensity initially increases with time, attains maximum value and then decreases for different mass of piston.

Fig.11 shows the variation of total ML intensity with mass of the sample. As mass of the sample increases ML intensity increases upto 15mg of sample and then remains constant.

It is suggested that barium based phosphor is strongly related to the movement of dislocations and the recombination of activated electrons and holes. The movements of dislocations excite carriers from the filled traps and the subsequent recombination of the electrons and holes occur in luminescence centers (Tb^{3+}).

5. THERMOLUMINESCENCE OF $BAALSI_5O_2N_7:TB^{3+}$

Fig. 12 shows typical glow curves for sample exposed to gamma rays 0.05 kGy at the dose rate of 0.3 kGy/hr. TL glow curves were taken for different concentration. The impurity (Eu) in the host material acts as emission centre in $BaAlSi_5O_2N_7$ host. The TL study on this material was not done. The shape of the glow peak remains almost similar with little shifting in the peak position for different concentrations of Tb. The shifting of peak towards higher temperature side is due to formation of high energy traps which are released at higher thermal energy[42]. The TL intensity goes on increasing from 0.05 mole% to 1 mole% of Tb and decreases for 2 mole%. This shows that samples gets quenched at 1 mole%. The presence of different type of trap due to γ irradiation effect is represented by TL glow curve. The prominent glow peak observed for different concentrations are 443K, 450K,441K,437K, 444K and 443K for 0.05, 0.1, 0.2, 0.5, 1 and 2 mole% respectively. All these low temperature peaks plays very useful role in thermoluminescence study of phosphor.

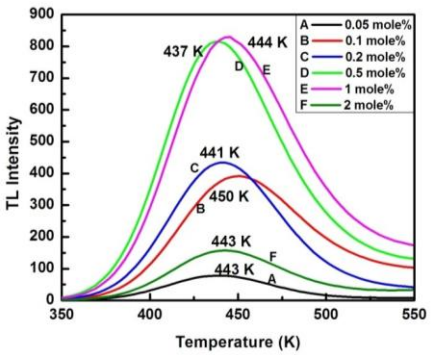

Fig. 12: TL glow curve of $BaAlSi_5O_2N_7:Tb^{3+}$ phosphor exposed to γ- ray of 0.05 kGy at the rate of 0.3 $kGyh^{-1}$

The study of TL glow curves with evaluation of trapping parameter associated with glow peak is one of the most important aspects of studies in the field of condensed matter physics. The dosimetric characteristics of any TL phosphor mainly depends on its trapping parameters which describe the defect centres responsible for TL emission. The various techniques have been developed for determination of trapping parameter as activation energy ***E***, order of kinetics ***b*** and frequency factor ***s.*** Various experimental techniques such as initial rise (IR) method, curve fitting methods, Chen's peak method, heating rate methods, isothermal decay analysis methods, etc. have been developed to determine these parameters from TL glow curves [43–47]. The TL process occurring in this material is explained in Fig.13. The ionization of phosphor occurs when the sample is irradiated with gamma ray. The free electrons are generated and trapped by electron traps/trap centers near the conduction band. The holes are trapped in luminescence centers near valence band. During readouts these trapped electrons are released from the trap centers and gain energy to reach the conduction band. When the electron comes in downward direction it recombines with luminescence centers and radiate energy in the form of photons (TL). From application point of view the simple glow structure with single peak is desirable [48]. In the present study the glow curve was studied by chen's peak shape method and Initial rise method.

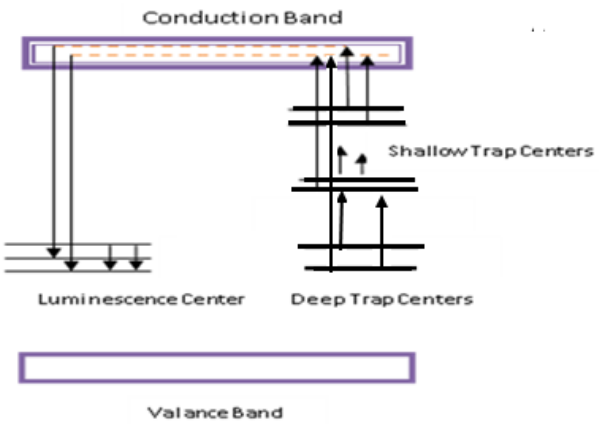

Fig. 13: Schematic multilevel TL model for competing trapping and luminescent centers[57]

5.1 Kinetic Study

5.1.1 Tm-Tstop Method

The number of glow peaks and position of glow peak present in glow curve was determined by Tm–Tstop method. The experimental glow curves were recorded for $BaAlSi_5O2N7$:Tb sample irradiated with 0.05 kGy dose of γ-particles from ^{60}Co source at the dose rate of 0.3 kGy/hr at different Tstop temperatures as shown Fig.14. This method involves heating of irradiated sample at a linear rate to some temperature Tstop. The sample was then cooled suddenly to room temperature and again

reheated so as to record the entire glow curve. The process is repeated many times with same irradiated sample but at different Tstop temperatures. When phosphor is heated to Tstop temperature, fraction of electrons is released from trapping states.

Therefore, during subsequent recording of the glow curve retrapping probability increases which results into shifting of Tm to high temperature side thereby decreasing the number of emitted photons and intensity of peak maxima. Fig. 14 depicts different Tm (maximum temperature of peak) steps when $BaAlSi_5O_2N_7:Tb^{3+}$ sample annealed after irradiation upto Tstop temperature from140 to 250^0C. Four steps are observed in the Tm temperatures when Tstop temperature varied from 140 to 250^0C. A single glow peak belongs to that region in which Tm remains nearly constant. Four such flat sectors can be distinguished in Fig. 14. We may sum up from the results obtained during study that the complex glow curve consists of four peaks at different temperatures.

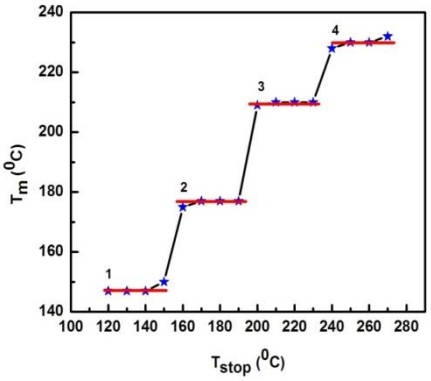

Fig. 14: Tm–Tstop plot for thermoluminescence glow curve of $BaAlSi_5O_2N_7:Tb^{3+}$ (1 mol%) phosphor

A complex glow curves was also analyzed by the computerized glow curve deconvolution (CGCD) method using TLANAL technique [49] in addition to the Tm–Tstop method to obtain the number of glow peaks.

5.1.2 Chen's Peak Shape Method

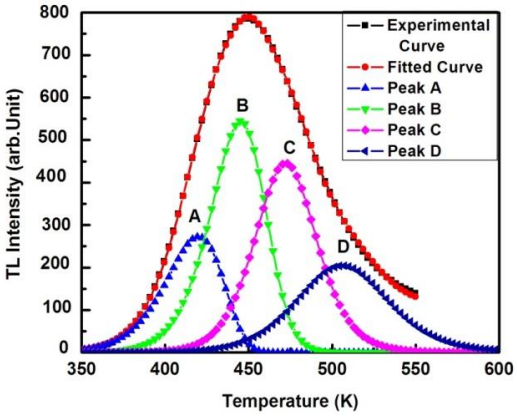

Fig. 15: Deconvoluted glow curves of $BaAlSi_5O_2N_7:Tb^{3+}$ phosphor

The $BaAlSi_5O_2N_7:Tb^{3+}$ phosphor glow-curve shows complex structure. So, the peak under the curve was separated by Tm-Tstop method. The parameters **E,s** and **b** were fitted to each peak. The curve fitting can be used only on the increasing side of peak and small amount on decreasing part, depending upon how well the peaks are separated. For deconvolution TLANAL software was used [50]. After deconvoluting glow curve, four isolated peaks are obtained (Fig.15). The glow curve was theoretically fitted by GCD method suggested by Kitis et.al [51]. It can be observed that four peaks are observed at 420K, 446K, 473K and 507K in the range 350 K to 550 K. This deconvoluted peak were found to follow first, second and general order kinetics in the host $BaAlSi_5O_2N_7:Tb$ [52]. The value of E i.e. trap depth was found to be 0.81 eV to 1.27 eV. The GCD functions for first, second and general orders of kinetics by Kitis et al [53] are:

For first order

$$I(T) = I_M \exp\left[\left(1+\left(\frac{E}{kT}\right)\left(\frac{T-T_M}{T_M}\right)\right) - \frac{T^2}{T_M^2}\left(1-\frac{2kT_M}{E}\right)\times\exp\left(\left(\frac{E}{kT}\right)\left(\frac{T-T_M}{T_M}\right)\right) - \frac{2kT_M}{E}\right] \quad (1)$$

For second order

$$I(T) = 4I_m \exp\left\{\left(\frac{E}{kT}\right)\frac{T-T_m}{T_m}\right\} \times\left[\left(\frac{T^2}{T_m^2}\right)\left(1-\frac{2kT}{E}\right) \exp\left(\frac{ET-T_m}{kTT_m}\right)+1+\frac{2kT_m}{E}\right]^{-2} \quad (2)$$

For general order,

$$I = I_m b^{(b-(b-1))}\exp\left(\frac{ET-T_m}{kTT_m}\right) \times\left[(b-1)\left(1-\frac{2kT_m}{E}\right)\frac{T^2}{T_m^2}\exp\left(\frac{ET-T_m}{kTT_m}\right) +1+(b-1)\frac{2kT_m}{E}\right]^{(b/(b-1))} \quad (3)$$

where *I(T)* is the TL intensity at temperature *T(K)*, I_m is the maximum peak intensity, *E* is the activation energy (eV), *k* is the Boltzmann constant and *b* is the order of

kinetics. The free parameters of the above GCD functions are the maximum peak intensity (I_m) and the maximum peak temperature (Tm), temperatures on both sides of the peak at half-intensities (T_1) and (T_2). All these quantities can be obtained experimentally from the glow peaks shown in Fig.16. Some authors suggested that the activation energy (E) and the order of kinetics (b) can be obtained experimentally [54].

The equations used in the glow curve shape method can be summarized as follows:

The activation energy (E)

$$E = c_\gamma\left(\frac{kT_m^2}{\gamma}\right) - b_\gamma(2kT_m) \tag{4}$$

In the above equation if γ is replaced by τ, δ, *or* ω then we get E_τ, E_δ *and* E_ω. The average of E_τ, E_δ and E_ω is E.

In equation (3) when γ is replaced by τ, δ, *or* ω then we get c_τ, c_δ, c_ω and b_τ, b_δ, b_ω which are the constants. k is the Boltzmann's constant and T_m is the maximum peak temperature. The values of c_τ, c_δ, c_ω and b_τ, b_δ, b_ω are summarized as below:

$$c_\omega = 3.54, c_\tau = 1.81, c_\delta = 1.71$$
$$b_\omega = 1, b_\tau = 2, b_\delta = 0$$

The frequency factor (s) for general order:

$$\frac{\beta E}{kT_m^2} = s\exp\left(\frac{-E}{kT_m}\right)\left[1+(b-1)\frac{2kT_m}{E}\right] \tag{5}$$

The values of c_γ and b_γ are summarized as below:

$$c_\tau = 1.51+(\mu_g - 0.42), b_\tau = 1.58+4.2(\mu_g - 0.42)$$
$$c_\delta = 0.976+7.3(\mu_g - 0.42), b_\delta = 0$$
$$c_\omega = 2.52+10.2(\mu_g - 0.42), b_\omega = 1 ----(5a)$$

The frequency factor (s) for First order

$$\frac{\beta E}{kT_m^2} = s\exp\left(\frac{-E}{kT_m}\right)$$

The values of c_γ and b_γ are summarized as below:

$$c_\tau = 1.51, b_\tau = 1.6$$
$$c_\delta = 0.98, b_\delta = 0 \tag{5b}$$
$$c_\omega = 3.54, b_\omega = 1$$

The frequency factor (s) for second order

$$\frac{\beta E}{kT_m^2} = s\exp\left(\frac{-E}{kT_m}\right)$$

The values of c_γ and b_γ are summarized as below:

$$c_\tau = 1.81, b_\tau = 2.0$$
$$c_\delta = 1.71, b_\delta = 0 \tag{5c}$$
$$c_\omega = 3.54, b_\omega = 1$$

where b is the order of kinetics, k is the Boltzmann constant and β is the linear heating rate (5^0Cs^{-1}).

The crystalline $BaAlSi_5O_2N_7:Tb^{3+}$ sample shows a broad TL emission glow curve. The experimental results can be fitted in good approximation by a four curve indicating the presence of four type of trap characteristic of microcrystalline samples. Fig.15 shows the results of deconvolution analysis. The peaks is centered at 420K, 446K, 473K and 507K. Peaks for $BaAlSi_5O_2N_7:Tb^{3+}$ were found to have kinetic order first order kinetics, second order kinetics and general order kinetics which also suggests retrapping probability of electrons. Further the kinetic trapping parameters namely, activation energy (E), frequency factor (s) and kinetic order (b) were determined from the deconvoluted glow curves by the above mentioned GCD functions. The normalized TL glow curve of $BaAlSi_5O_2N_7:Tb^{3+}$ phosphor for individual peaks are shown in Fig 14. The kinetic parameters of $BaAlSi_5O_2N_7:Tb^{3+}$ phosphors for individual peaks are shown in Table 1. FOM for $BaAlSi_5O_2N_7:Tb^{3+}$ is equal to 1.03%. This result indicates the good result of deconvolution process. The figure of merit (FOM) of fitting has also been determined using the formula [55]

$$FOM = \frac{\sum_i (TL_{Exp} - TL_{fit})}{\sum_i TL_{fit}} \times 100\% \tag{6}$$

where TL_{Exp} and TL_{fit} represent the experimental TL intensity data and the values of the fitting functions, respectively. Here summation extends over all the available experimental data points

5.2 Initial Rise Method

The initial rise method is another method of analysis of TL parameter. This method of analysis was first suggested by Garlick and Gibson [56].This experimental method is applicable to any order of kinetics and is based on the analysis of the low temperature interval of a peak. As per initial rise method the amount of trapped electrons in the low temperature tail of a TL glow peak can be assumed to be approximately constant because $n(T)$ is independent of temperature T in that temperature region. This remains true for temperatures up to a cutoff temperature T_C, corresponding to a TL intensity I_C smaller than about 15% of the maximum TL intensity I_M.

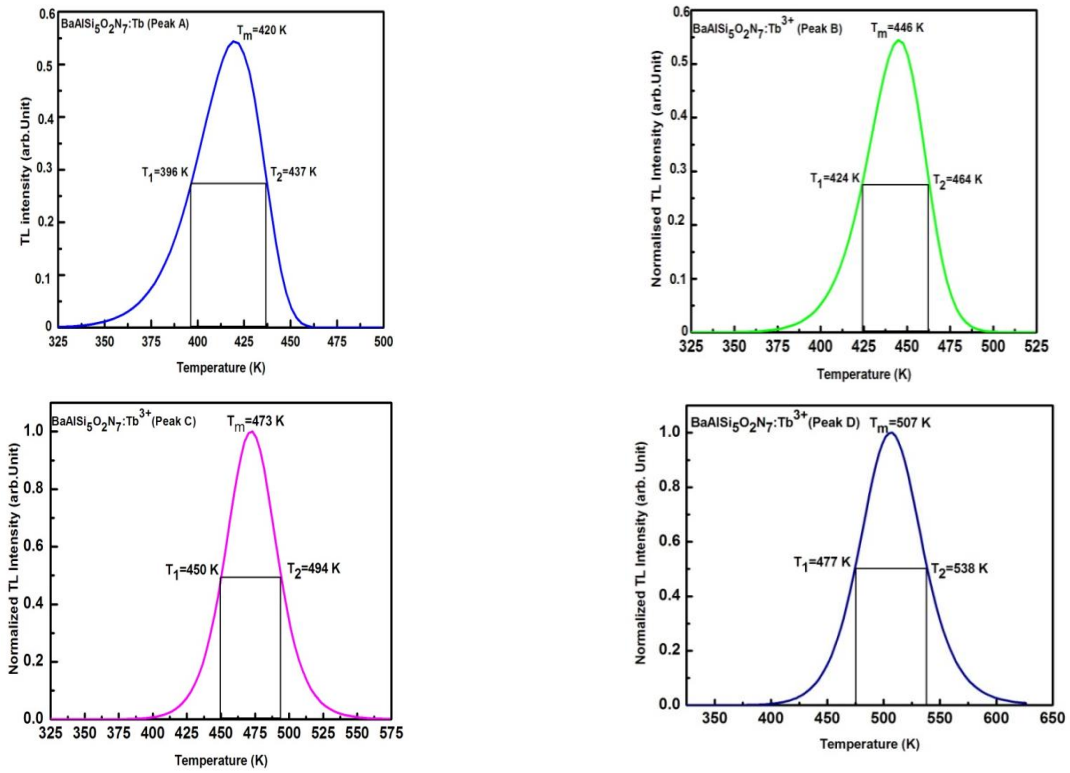

Fig. 16:. Normalized TL glow curve showing parameters T1, T2, Tm for Chen's peak shape method

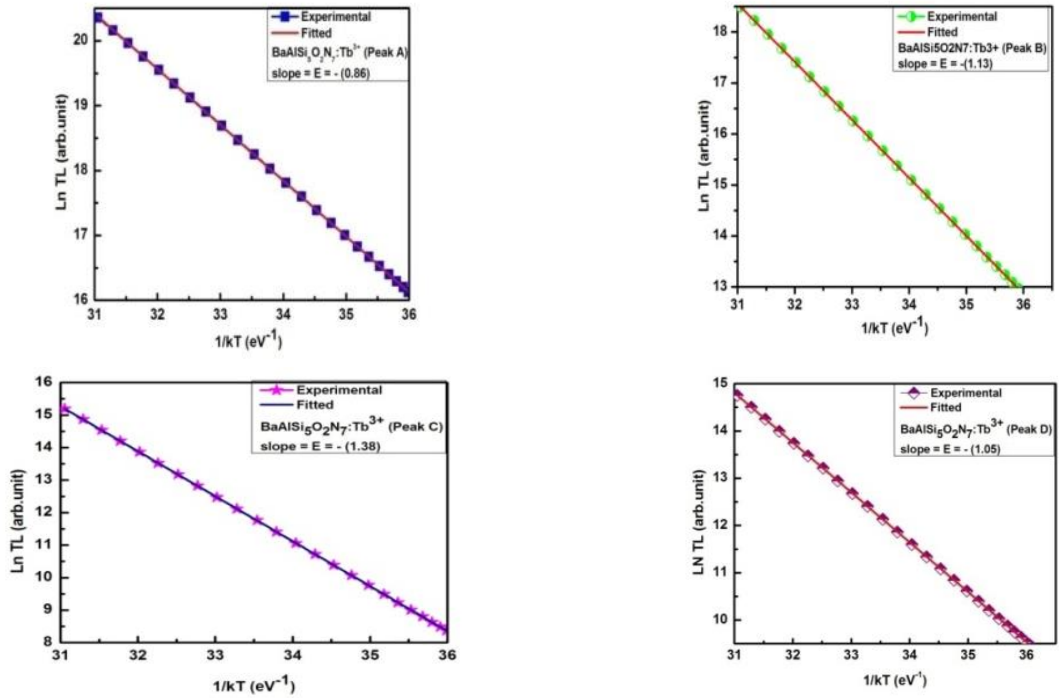

Fig. 17: Initial rise plot of ln(TL) versus 1/KT of $baAlSi_5O_2N_7:Tb^{3+}$

The TL intensity I(T)is given as-

$$I(T) = Ce^{(\frac{-E}{kT})}$$

Where C is the constant, I(T) is the TL intensity at any temperature T.

When the sample is heated at a linear heating rate of b = dT/dt, E is the thermal activation energy and k is Boltzmann's onstant. A plot of 1/kT versus ln(TL) over the initial rise region gives a straight line and from the slope -E/k, activation energy E(eV) can be calculated (Fig.17). The important necessity for this initial rise

Table 1: Kinetic parameters of $BaAlSi_5O_2N_7:Tb^{3+}$ using Chen's peak method

Phosphor	*Peak No.*	*T_1 (K)*	*T_2 (K)*	*T_m (K)*	*Order of kinetics (b)*	*Geometrical form factor (μ_g)*	*Activation energy (eV)*	*Frequency factors (s^{-1})*
$BaAlSi_5O_2N_7:Tb^{3+}$	A	420	395	438	1	0.42	0.81	1.68×10^9
	B	446	424	464	1.3	0.45	1.13	7.38×10^{11}
	C	477	450	449	1.5	0.48	1.27	4.76×10^{12}
	D	477	538	507	2	0.50	1.19	2.32×10^{11}

Table 2: Comparison of kinetic parameters by Chen's peak shape method and Initial rise method

Phosphor name	*Method*	*Peak No.*	*E(eV)*	*$S(s^{-1})$*
$BaAlSi_5O_2N_7:Tb^{3+}$	Chen's peak shape	A	0.81	1.68×10^9
		B	1.13	7.38×10^{11}
		C	1.27	4.76×10^{12}
		D	1.19	2.32×10^{11}
	Initial rise	A	0.86	1.38×10^{21}
		B	1.13	1.19×10^{24}
		C	1.38	5.92×10^{23}
		D	1.05	2.12×10^{21}

analysis is assumption that the concentration of the trapped carriers remains approximately constant at any instant. But this assumption becomes invalid beyond the cut-off temperature. By this method E is found to be 0.86 eV to 1.38 eV.

6. CONCLUSIONS

In this paper the samples were synthesized by high temperature modified two step solid state diffusion methods. The luminescence properties of Tb^{3+} in the $BaAlSi_5O_2N_7$ sample were investigated. In excitation spectrum several sharp peaks were observed. With increasing Tb^{3+} content emission intensity increases from 0.05 mole% to 1 mole% and then decreases, suggesting that concentration quenching occurs at 1 mole%. The emission spectra exhibit a major peak at 544 nm attributed to $^5D_4$ to $^7F_5$ transition of Tb^{3+} in green region. The critical transfer distance of Tb^{3+} in $BaAlSi_5O_2N_7:Tb^{3+}$ was found to be 33.39Å. From excitation and emission spectra, $BaAlSi_5O_2N_7:Tb^{3+}$ phosphors can be effectively excited by UV light (270 nm) and exhibited a satisfactory green emission (544 nm) thus widely applied as UV LED chip.

ML intensity increases with increasing concentration of impurity.When load is applied on the sample, initially the ML intensity increases with time, attains a peak value I_m at a particular time t_m and later on it decreases with time. Intensity also increases with height through which the load is dropped on the sample. When the sample is deformed elastically by dropping a load of small mass from a low height then initially the ML intensity increases with time, attains a peak value and later on it decreases with time. Intensity increases with height through which the load is dropped on the sample. ML intensity increases linearly with the density of filled hole traps. The trapping and detrapping of charge carriers in the material can be studied using ML. This fundamental work might be important in developing new luminescent devices applicable for ML sensors and dosimeter

In thermoluminescence study, the peak was separated by Tm-Tstop technique. Glow curve of γ-irradiated $BaAlSi_5O_2N_7:Tb^{3+}$phosphor show four peaks at temperatures 420K, 446K, 473K and 507K indicating that four type of traps are formed. The trapping parameter i.e. activation energy (E) and frequency factor (S) were calculated bychen's peak shape method and initial rise method.Maximum TL intensitywas found for 1 mole% of Tb^{3+} ion.The glow curves were theoretically fitted by GCD function.The glow curves follows the first, second and general order kinetics which is calculated by peak shape method.The activation energy and frequency factor are calculated by both the methodsshow good proximity with each other.

REFERENCES

[1] S.Ye, F.Xiao, Y.X. Pan, Y.Y. Ma, Q.Y. Zhang, Materials Science and Engineering R71(2010) 1.

[2] K. Sakuma, N. Hirosaki, and R. Xie, J. Lumin. 126 (2007) 843

[3] S. Yao and D. Chen, J. Opt. Laser Technol. 40 (2008) 366.

[4] S.J. Yoon, S.J. Dhoble, K. Park Ceramics International 40 (2014) 4345.

[5] H.A.A.S. Ahmed, O.M. Ntwaeaborwa, R.E. Kroon, Journal of Luminescence 135 (2013) 15.

[6] R.-J. Xie, N. Hirosaki, Sci. Technol. Adv. Mater. 8 (2007) 588

[7] Y.Q. Li, J.E.J. van Steen, J.W.H. van Krevel, G. Botty Naito T. Nakajima, H. Yamamoto, Electrochem. A.C.A. Delsing,, F.J. DiSalvo, G. de With, H.T. Hintzen, J. Alloys Compd. 417 (2006) 273.

[8] Y.Q. Li, G. de With, H.T. Hintzen, J. Solid State Chem. 181 (2008) 515.

[9] Y.Q. Li, N. Hirosaki, R.J. Xie, T. Takeda, M. Mitomo, Chem.Mater. 20 (2008) 6704.

[10] K. Uheda, N. Hirosaki, Y. Yamamoto, A. Solid-State Lett. 9 (2006) 4.

[11] K. Uheda, N. Hirosaki, Y. Yamamoto, H. Yamamoto Phys. Stat. Sol. A 203 (2006)2712

[12] H. Watanabe, H. Yamane, N. Kijima, J. Solid State. Chem. 182 (2008) 1848.

[13] H. Watanabe, N. Kijima, J. Alloys Compd. 475 (2008) 434.

[14] D.H. Gregory, J. Chem. Soc., Dalton Trans. (1999) 259.

[15] W. Schnick, H. Huppertz, Chem. Eur. J. 3 (1997) 679.

[16] R. Marchand, F. Tessier, A. Le Sauze, N. Diot, Int. J. Inorg. Mater. 3 (2001) 1143.

[17] W. Schnick, Angew. Chem. Int. Ed. Engl. 32 (1993) 806;

[18] R. Niewa, F.J. DiSalvo, Chem. Mater. 10 (1998) 2733.

[19] J.W.H. van Krevel, H.T. Hintzen, R. Metselaar, A. Meijerink, JAlloys Compd. 268 (1998) 272.

[20] S.C. Gedam, S.J. Dhoble, S.V. Moharil, Journal of Luminescence 126 (2007) 121.

[21] V. Natarajan, A.R. Dhobale, C.H. Lu, Journal of Luminescence 129 (2009) 290.

[22] J.-Y. Park, H.-C. Jung, G.S.-R. Raju, B.-K. Moon, J.-H. Jeong, J.-H. Kim, Journal of Luminescence 130 (2010) 478.

[23] S.P. Khatkar, S.D. Han, V.B. Taxak, G. Sharma, D. Kumar, Optical Materials 29 (2007) 1362.

[24] S. Lian, Y. Qi, C. Rong, L. Yu, A. Zhu, D. Yin, and S. Liu, J. Phys. Chem. C 114(15) (2010)7196.

[25] B. P. Chandra, edited by D. R. Vij (Plenum Press, 1988), 361.

[26] C. N. Xu, T. Watanabe, M. Akiyama, and X. G. Zheng, Appl. Phys. Lett. 74(9), (1999)1236.

[27] X. Wang, C. N. Xu, H. Yamada, K. Nishikubo, and X. G. Zheng, Adv. Mater. 17(10),(2005) 1254.

[28] C. N. Xu, T. Watanabe, M. Akiyama, and X. G. Zheng, Appl. Phys. Lett. 74(17) (1999) 2414.

[29] S. Kamimura, H. Yamada, and C. N. XuAppl. Phys. Lett. 101(9) (2012) 091113.

[30] J. Botterman, K. V. Eeckhout, I. D. Baere, D. Poelman, and P. F. Smet, Acta Mater. 60(15) (2012) 5494.

[31] J. C. Zhang, X. Wang, X. Yao, C. N. Xu, and H. Yamada, J. Electrochem. Soc. 157(12) (2010) G269.

[32] Azorı´n,J.,Furetta,C,Scacco,A Physica Status Solidi A138(1),(1993)9.

[33] Nameeta Brahme, D.P.Bisen, R.S. Kher, M.S.K Khokhar. Physics Procedia 2 (2009) 431.

[34] C.J. Duan, W.M.Otten, A.C.A.Delsing, H.T.Hintzen. J. Alloys and Comp. 461 (2008) 454.

[35] Dr.J.Cooke,Department of chemistry,University of Alberta,2005

[36] Dongling Geng, Hongzhou Lian, Mengmeng Shang, Yang Zhang, and Jun Lin journal of inorg.Chem.53 (2014)2230

[37] P. Li, L. Pang, Z. Wang, Z. Yang, Q. Guo, X. Li, Journal of Alloys and Compounds 478 (2009) 813.

[38] X. Zhang, X. Qiao, H.J. Seo, Journal of the Electrochemical Society 157 (2010) J267.

[39] C. N. Xu, T. Watanabe, M. Akiyama, and X. G. Zheng Appl. Phys. Lett. 74(17), (1999) 2414.

[40] B. Chen, J. Yu, X. Liang, Langmuir 27 (2011) 11654.

[41] Zhijun Zhang,Otmar M.ten Kate,Anneke Delsing,Erik van der Kolk,Peter.H.L.Notten,Pieter Dorenbos,Jingtai Zhao and Hubertus T.Hintzen Journal of Mater. Chem.22(2012)9813.

[42] A.J.J. Bos Radiation Measurements 41 (2007) S45.

[43] S.W.S. McKeever, (1985). Thermoluminescence of Solids, Cambridge University Press, p.75.

[44] J. Azorin, C. Furetta, and A. Gutierrez, J. Phys. D: Appl. Phys.22 (1989) 458.

[45] Y. Kirsh, Phys. Stat. Sol. A 129 (1992), 15.

[46] S.W.S. McKeever,. Nucl. Instrum. Methods 175 (1980),19.

[47] G.C. Taylor, and E. Lilley, J. Phys. D: Appl. Phys. 11 (1978) 567.

[48] Manveer Singh, P.D. Sahare, Pratik Kumar Radiation Measurements 59 (2013) 8.

[49] S. Som, M. Chowdhury, S.K. Sharma J. Radiation Physics and Chemistry 110(2015)51.

[50] K. S. Chung, H. S. Choe, J. I. Lee, J. L. Kim and S. Y. Chang J. Radiation Protection Dosimetry 115 (2005), 345.

[51] B. P. Kore, N.S.Dhoble and S.J. Dhoble J. Lumin. 145 (2014) 888.

[52] Numan Salah, Zishan H. Khan, Sami S. Habibet, J.Nucl. Instr. and Methods in Phys. Res. B 269 (2011) 401.

[53] G. Kitis, J.M. Gomez-Ros, J.W.N. Tuyn, J. Phys. D: Appl. Phys. 31 (1998) 2636.

[54] V. Pagonis, G. Kitis, C. Furetta, Numer. Pract. Exercises Thermolumin. (2005).

[55] M. Singh, P.D. Sahare, P. Kumar, Radiat. Measur. 59(2013)8.

[56] G.F.J. Garlick, and A.F. Gibson,. Proc. Phys. Soc. Lond. 60 (1948) 574.

[57] S.A.fartode, Vijay Singh and S.J.Dhoble Defect and Diffusion Forum 361(2015)177